Volume 6, Issue 4, 2016, 1422-1427 ISSN 2069-5837

Biointerface Research in Applied Chemistry

www.BiointerfaceResearch.com

Original Research Article Open Access Journal

Received: 27.04.2016 / Revised: 25.06.2016 / Accepted: 10.07.2016 / Published on-line: 20.07.2017

Discriminating between active and inactive compounds using binding energy calculations – a case study

Smriti Khanna [1], Chandrika B-Rao [1,*], Usha Ghosh [2], Zejah Rizvi [2], Komal Bajaj [2], Asha Kulkarni-Almeida [3], Rajiv Sharma [2]

[1]Discovery Informatics, Piramal Enterprises Limited, Goregaon (E), Mumbai 400 063, Maharashtra, India
[2]Department of Medicinal Chemistry, Piramal Enterprises Limited, Goregaon (E), Mumbai 400 063, Maharashtra, India
[3]Department of High Throughput Screening and Biotechnology, Piramal Enterprises Limited, Goregaon (E), Mumbai 400 063, Maharashtra, India
*corresponding author e-mail address: ***chbrao@hotmail.com***

ABSTRACT

Xanthine oxidase inhibitors fall into two classes, those which co-ordinate to molybdopterin cofactor (e.g. allopurinol) and those which do not (e.g. febuxostat). Recently we discovered a novel pyrimidine-containing scaffold, isocytosine, exhibiting nanomolar IC_{50} values in enzymatic assays. Molecular docking studies showed binding pattern similar to that of febuxostat. Shifting a nitrogen atom in the pyrimidine ring (for convenience we will call them 'reverse pyrimidine' analogs), and docking to xanthine oxidase gave similar interactions and docking scores for the two chemotypes. However, the reverse pyrimidines showed loss of activity when tested in enzymatic assay. As docking studies did not discriminate between the two scaffolds, in an effort to explain this unexpected result from the enzymatic assay, MMGB-SA binding energy calculations were done on docked complexes. Detailed analysis of various contributing energy terms to deltaG values from MMGB-SA calculations indicated that the 'ligand-in-complex' energy values consistently differ by ~20 kcal/mol between pairs of pyrimidine and corresponding reverse pyrimidine derivatives. Ligand-in-complex energy values are a measure of stability of bound ligand to the protein active site. Higher values of this energy term for reverse pyrimidines suggest that this chemotype, when bound in the receptor environment, has unfavorable contacts that may be responsible for the reduced activity of these compounds. From this study it can be inferred that MMGB-SA binding energy calculations may be used as an alternative when docking studies do not provide expected results.

KEYWORDS: xanthine oxidase inhibitors, docking, isocytosine, MMGB-SA, binding energy, ligand strain.

1. INTRODUCTION

Xanthine oxidoreductase (XOR) is an important metalloprotein and one of the various oxidoreductases present in any organism. It is a homodimeric protein of 290kDa [1]. It occurs in two interconvertible forms: oxidase and dehydrogenase [2]. As the name suggests, it carries out some vital oxidation-reduction reactions [3]. In its capacity as an oxidoreductase, it catalyzes hydroxylation of purine substrates like hypoxanthine to xanthine to uric acid [4]. Uric acid is the final metabolite in the purine metabolism pathway in humans and is excreted as such [5]. However, in most mammals, uric acid is further converted to a more water-soluble form, allantoin, by the enzyme uricase which does not exist in humans [2]. Excessive accumulation of uric acid in blood serum leads to hyperuricaemia which raises the risk of the disease, gout [6, 7]. The class of compounds called xanthine oxidase inhibitors (XOIs) blocks the synthesis of uric acid by inhibiting XOR and is used in the treatment of hyperuricemia-related disorders like gout.

Allopurinol [8, 9] and febuxostat [10] are the most important drugs in this class [11]. Allopurinol was the first XOI that reached the market in 1964 and has monopolized it for half a century now [12]. The second XOI to gain US FDA approval in 2009 was febuxostat, although it was approved a year earlier by EMA [12]. The two drugs differ in their mechanisms of action. Allopurinol is a substrate analog of hypoxanthine. Within two hours of oral administration, it is metabolized through hydroxylation by xanthine oxidase to its active metabolite oxypurinol, which is also an XOI and binds irreversibly in the hypoxanthine binding site. Allopurinol interferes in purine-pyrimidine metabolism and hence has serious side-effects resulting even in death in some rare cases. Febuxostat is a non-purine non-substrate inhibitor that does not get metabolized by XOR [13, 14]. However it has hepatotoxicity effects in some patients and was recommended only as a second line of treatment after allopurinol in the USA. Keeping in mind the side effects associated with these agents, the current situation indeed warrants design and development of new non-purine inhibitors. Recently isocytosine was discovered as a novel scaffold possessing xanthine oxidase inhibitory activity by our group [15]. A virtual screening project using PASS (Prediction of Activity Spectra of Substances) [16] predictions for xanthine oxidase inhibition on in-house synthetic library unveiled an initial hit containing isocytosine moiety with micromolar activity in enzymatic xanthine oxidase inhibition assay. Many designed compounds were virtually docked, synthesized and tested [17, 18]. For most of the designed compounds, results from in vitro experiments matched the predictions from docking but some did not. In the current study, one such case is reported where a series of compounds predicted as XOIs by docking studies did not show the expected results in enzymatic assay. This set of compounds, which were found to be false positives from docking, were analyzed further with additional computational studies in an effort to rationalize the observed in vitro results.

2. EXPERIMENTAL SECTION

2.1. Computational Analysis.

Molecular docking studies were carried out using GLIDE [19] module of Schrodinger Suite of programs. XOR with PDB code 1VDV co-crystallized with piraxostat was employed for docking [20]. It was selected from all the XOR crystal structures available in PDB based on various crystal structure parameters like resolution, B-factor and R-values, completeness of structure etc. The protein used for docking was prepared by "Protein Preparation Wizard" of Schrodinger Suite. All the molecules to be docked were sketched within maestro using the BUILD module of Schrodinger Suite. The sketched molecules were prepared for docking using the LIGPREP module of Schrodinger. All the ionized and tautomeric forms generated by LIGPREP were docked including the keto and the enol forms, protonated and deprotonated forms. For performing the docking studies, active site grid was defined as a box of size 10Å x 10Å x 10Å around the centroid of the ligand piraxostat. Within GLIDE, rigid docking protocol as implemented in extra-precision (XP) mode was employed.

2.2. In vitro enzymatic assay.

The in vitro assay was set up based on protocols reported in literature [21]. The assay was standardized using the Tecan system with the integrated Safire 2 reader to run it in high throughput screening (HTS) mode. 96 well UV transparent plates from Corning Life Sciences, USA, were used in the Jasco spectrophotometer. In the current set up, the absorption peak of uric acid was found at 310 nm. At this wavelength a linearly increasing trend was observed for absorbance with increasing concentrations of uric acid. Xanthine oxidase (XO) activity was monitored spectrophotometrically on the HTS system following the absorbance of uric acid at 310 nm under aerobic condition.

The XO activity was observed in presence of varied concentrations of bovine XO (Calbiochem) and xanthine (Sigma). The concentrations at which the formation of uric acid stabilized were found to be 200 mU XO and 400 μM xanthine at 30 min. These parameters were used for further screening. The enzyme solution of XO prepared in water was added to the test compounds or vehicle control (0.5% DMSO). The reaction was initiated by addition of xanthine in 50 mM potassium phosphate buffer (pH 7.5) as the substrate to the above assay mixture. The absorbance at 310 nm, indicating the formation of uric acid, was measured at 30 min at ambient temperature. Assays were repeated three times. Allopurinol was used as positive control. The inhibitory activity of each test compound against XO was indicated by their IC_{50} values.

3. RESULTS SECTION

3.1. Computational studies and synthesis of Reverse pyrimidines.

PASS based virtual screening identified an initial hit (compound 1, Figure 1) containing isocytosine moiety with an IC_{50} of 9.4 μM in enzymatic xanthine oxidase inhibition assay. Various modifications of compound 1 were designed by structure-based approach, leading to a number of compounds with nanomolar activity [17, 18]. Overall docking predictions based on docking scores, pose and interactions showed an accuracy of ~81%. Some of the designs which turned out to be false positives were thoroughly studied and analyzed to elucidate possible reasons for inactivity. As a part of the lead generation process, different core modifications were attempted to obtain novel scaffolds. One such modification was changing the position of pyrimidine ring nitrogen in isocytosine to generate the 'reverse pyrimidine' moiety (Figure 1). While one of these nitrogens in pyrimidine ring was actively engaged in forming H-bonds with the receptor active site residue Glu802, the other did not show any interactions with the protein (Figure 2). The nitrogen which formed H-bond was retained while the other nitrogen was shifted to the alternate pyrimidine position. Four such sets of compounds with pyrimidines and corresponding reverse pyrimidines were docked to the active site of XOR (PDB code 1VDV) which is co-crystallized with piraxostat, [22] a structural analog of febuxostat, using GLIDE module of Schrodinger Suite of programs. Both keto and enol tautomers were docked for the first 3 pairs (1, 2; 3, 4 and 5, 6). Analysis of the docked poses showed that pyrimidine as well as reverse pyrimidine derivatives occupied the same space in the active site, had equivalent dock scores and similar interactions.

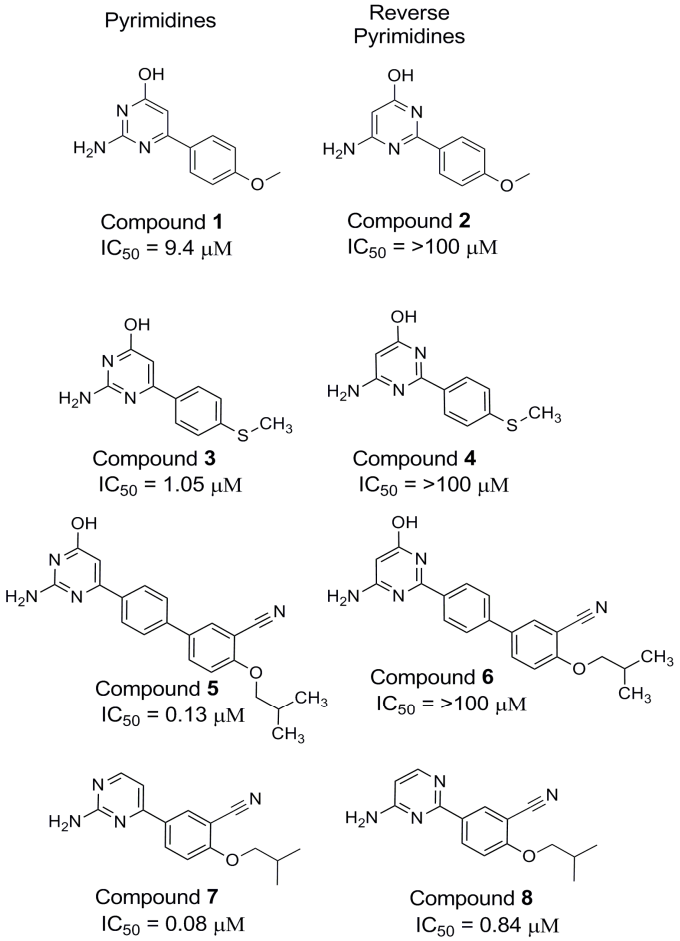

Figure 1. Compound 1 is the virtual screening hit used for structure-based drug design. Compound 2 is its reverse pyrimidine analog. IC_{50} values from xanthine oxidase inhibition assay indicate reduced activity of reverse pyrimidine analogs for all 4 pairs.

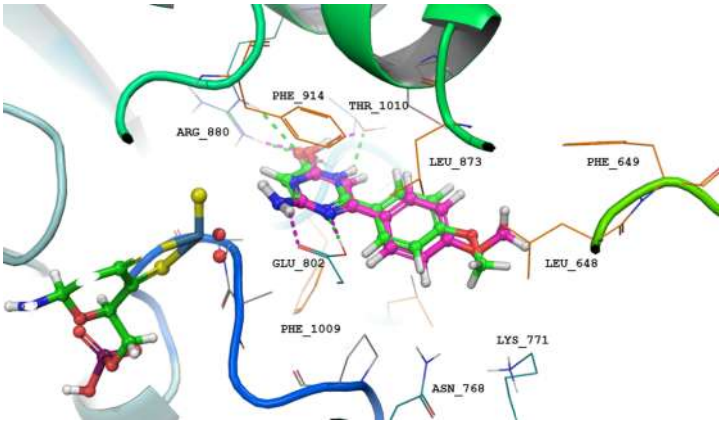

Figure 2. Docked poses of compounds **1** (magenta) and **2** (green). **2** shows an additional H-bond between –NH of amide (in the keto form) and Thr1010.

Although the -NH group of reverse pyrimidines in the keto form showed an additional H-bond with protein residue Thr1010, not observed in isocytosine analogs (Figure 2), enol form for both the chemotypes showed better dock scores (Table 1). Supported by docking studies, all eight compounds were synthesized. The synthesized compounds were tested in a high throughput enzymatic assay to check xanthine oxidase inhibitory potency by measuring reduction of uric acid based on UV absorption read-outs. The enzymatic assay results turned out to be quite surprising as pyrimidine derivatives showed potent activity but the corresponding reverse pyrimidines were either inactive (compounds 2, 4 and 6) or substantially less active (compound 8, which lacked hydroxyl group).

Table 1. Activity, Dock scores, 'ligand-in-complex' energies from MMGB-SA, dGp-rp values for all the compounds.

			Force field based		Quantum based	
ID	**IC_{50} (□M)**	**Dock Score**	**Ligand-in-Complex Energy**	**dG_{p-rp}**	**Ligand-in-Complex Energy**	**dG_{p-rp}**
1-Enol	9.4	-12.60	-140.86	-18.97	-139.13	-17.65
2-Enol	>100	-12.68	-121.89		-121.48	
3-Enol	1.05	-13.03	-143.00	-18.02	-142.79	-17.03
4-Enol	>100	-11.95	-124.98		-125.76	
5-Enol	0.13	-14.22	-124.22	-22.48	-123.46	-17.55
6-Enol	>100	-14.16	-101.73		-105.90	
7	0.078	-12.20	-114.92	-10.89	-121.17	-12.85
8	0.84	-10.94	-104.03		-108.33	
ID	**IC_{50} (□M)**	**Dock Score**	**Ligand-in-Complex Energy**	**dG_{p-rp}**	**Ligand-in-Complex Energy**	**dG_{p-rp}**
1-Keto	9.4	-10.36	-26.53	-17.99	-27.17	-17.42
2-Keto	>100	-12.11	-8.54		-9.75	
3-Keto	1.05	-9.75	-27.93	-17.69	-33.01	-20.16
4-Keto	>100	-12.48	-10.25		-12.85	
5-Keto	>100	-11.96	-9.73	-17.38	-12.66	-18.01
6-Keto	>100	-13.93	7.65		5.35	
7	0.078	-12.20	-114.92	-10.89	-121.17	-12.85
8	0.84	-10.94	-104.03		-108.33	

Dock scores and other energy terms in kcal/mol, dGp-rp: Difference of Ligand-in-Complex energy for pyrimidine and reverse pyrimidines pairs

3.2. MMGB-SA calculations.

It is well-known that while scoring functions give a general idea of strength of binding, and usually enable prediction of the correct pose of ligand in the active site of protein, they do not correlate well with experimentally observed binding affinity data. Here, we assume that the relative IC_{50} values indicate relative binding affinities. Better estimates of binding strength between ligand and protein for a given ligand pose can be obtained using more complex energy calculations. Towards this end, on all the eight docked complexes, MMGB-SA binding energy calculations were done as implemented in PRIME module [23] of Schrodinger. The protein active site within a sphere of 10Å around the docked ligand was kept flexible except for the molybdopterin (Mo-Pt) cofactor while calculating energy values.

Charges were calculated in two ways. In the first method, force field based OPLS-2005 charges were assigned to the ligand. For more accurate results, quantum mechanics B3LYP-lacvp* charges were calculated separately and incorporated into the ligand before performing MMGB-SA calculations. Quantum mechanics based charges are expected to give more accurate estimate of electrostatics than force field based methods. A comparison of the energy terms obtained from both the calculations is shown in Table 1. None of the energy terms, dG1 (receptor and ligand strain energy together), dG2 (receptor strain only), dG3 (ligand strain alone) and dG4 (overall binding energy of the docked complex) showed any direct correlation with the observed activities. The various contributing energy terms to the complex energy such as electrostatic and hydrophobic terms, solvation effects and strain energies were also examined. Of all the

terms, the most evident difference between the two chemotypes was observed for the term 'ligand-in-complex' energy, which represents stability of ligand within protein active site environment. Lower the values of 'ligand-in-complex' energy, more suitable is the protein environment and better the ligand placement in the active site. For the first three pairs, pyrimidine analogs were ~18-22 kcal/mol more stable than the reverse pyrimidine analogs using both the methods. The last pair of compounds gave lower difference of 10-12 kcal/mol which reflects the 10-fold reduced activity of compound 8 versus 7. Higher values for 'ligand-in-complex' energy for reverse pyrimidines than pyrimidines, indicate existence of certain destabilizing factors for reverse pyrimidines in the protein active site environment which are not visually detectable and which are not captured by the docking algorithm either. The ligands in this form experience some unfavorable contacts when complexed with protein due to which there is tremendous loss in potency. Ligand strain is not very uncommon in co-crystallized ligands. In fact, most ligands when complexed to protein do experience some strain which is within acceptable range. In the current scenario, the ligand conformation perhaps results in strain which is quite severe resulting in less stable complexes with consequent loss in potency.

3.3. Strain Energies.

To further support the hypothesis, alternate strain energy values for the docked poses of the ligands were generated using quantum chemical methods in different steps. In the first step, ligands in their docked conformations were extracted from the docked ligand-protein complexes and subjected to single point energy (SPE) calculations using B3LYP method with 6-31G** basis set as implemented in JAGUAR module [24] of Schrodinger. SPE values gave energies of the ligands independent of the protein but in the same conformations as they were found when complexed with the protein. In the next step, complete optimization of the same ligands was done in the absence of the protein. Full optimization energies (FOE) thus obtained gave energies of the ligands free from all kinds of protein confinements. The strain energies were calculated from SPE and FOE as below.

$$\text{Strain Energy} = \text{SPE} - \text{FOE}$$

The strain energies thus obtained for all the compounds were analyzed (Table 2). For the enol form the strain energies were found to be almost equivalent for pairs of pyrimidines and reverse pyrimidines. But the real difference was observed for the keto forms where the strain energy was found to be much more pronounced for all reverse pyrimidines (~10 kcal/mol) compared to pyrimidines except the last pair (~4 kcal/mol) where keto-enol tautomerism is not present.

Table 2. Single point energies (SPE), full optimization energies (FOE) and strain energies (SE) calculated for all the compounds.

Title	SPE	FOE	SE	dSEp-rp
1-Enol	-464671.3139	-464682.6371	11.32	-1.35
2-Enol	-464674.9528	-464687.6301	12.68	
3-Enol	-667339.3306	-667351.3974	12.07	-0.74
4-Enol	-667343.6578	-667356.4651	12.81	
5-Enol	-741554.358	-741573.4785	19.12	0.89
6-Enol	-741560.4102	-741578.6441	18.23	
7	-549364.3093	-549371.4176	7.11	-4.26
8	-549364.1719	-549375.5397	11.37	
Title	**SPE**	**FOE**	**SE**	**dSEp-rp**
1-Keto	-464671.7563	-464685.912	14.16	-11.67
2-Keto	-464661.2714	-464687.0993	25.83	
3-Keto	-667339.5527	-667354.7037	15.15	-11.11
4-Keto	-667329.3295	-667355.5891	26.26	
5-Keto	-741555.3751	-741576.8206	21.45	-10.39
6-Keto	-741545.4945	-741577.3301	31.84	
7	-549364.3093	-549371.4176	7.11	-4.26
8	-549364.1719	-549375.5397	11.37	

dSEp-rp : Difference of SE for pyrimidine and reverse pyrimidine pairs in kcal/mol

3.4. Conformational landscapes.

Additionally, conformational energy landscape was generated by scanning torsion angle connecting the heterocyclic ring with the phenyl ring for every 10° rotation. This was done using B3LYP method with 6-31G** basis set implemented in JAGUAR module. The highest energy conformations had the two rings perpendicular to each other (90°) for both the chemotypes (Table 3). The lowest energy conformations for enol and keto forms for pyrimidines and only the keto form for the reverse pyrimidines showed a deviation of ~20° from planarity which can be attributed to the steric clash of the ortho hydrogens on the two rings. The difference in energies between the highest and lowest energy conformers was ~5 kcal/mol for all the three species. However, this difference was found to be higher for the enol form

of the reverse pyrimidines (~8 kcal/mol) where the most stable conformation was found to be completely planar (absence of ortho hydrogens). This leads to the inference that the enol form of the reverse pyrimidines has more stringent conformational preferences than the keto form and that can also lead to higher degree of strain as their docked poses are not planar.

Thus strain energy calculations show keto form to be more strained when bound to the receptor and the torsion scan drive indicates enol form to be more restrictive in terms of binding conformations. In either case the reverse pyrimidines seem to show some concerns related to strain energy which are not observed in pyrimidine derivatives. Considering equal probability of binding for enol and keto forms for all the ligands to the receptor, pyrimidine derivatives have a greater chance of showing better binding affinity as both forms show equivalent energy parameters. But the same may not hold true for reverse pyrimidines as both forms experience some sort of strain as indicated by the different energy calculations shown here and it may be less likely for them to bind as strongly to the receptor as the pyrimidine derivatives except for the last pair of compounds where keto-enol tautomerism does not exist. Compound 8 is the only example in the reverse pyrimidine derivatives which is not completely inactive but has shown 10-fold reduction in activity than its pyrimidine counterpart compound 7.

Table 3. Torsion angles of lowest and highest energy conformations, and their energy differences calculated for all the compounds.

Title	TA-LowE	TA-HigE	dE (kcal/mol)
1-Enol	160	90	5.28
2-Enol	180	90	8.61
3-Enol	160	90	5.17
4-Enol	180	90	8.57
5-Enol	160	90	4.55
6-Enol	180	90	8.06
7	20	90	5.46
8	0	90	8.98
Title	**TA-LowE**	**TA-HigE**	**dE (kcal/mol)**
1-Keto	20	90	5.29
2-Keto	160	90	5.90
3-Keto	20	90	5.48
4-Keto	180	90	5.95
5-Keto	30	90	4.81
6-Keto	160	90	5.44
7	20	90	5.46
8	0	90	8.98

TA-LowE: Torsion angle of the lowest energy conformer
TA-HigE: Torsion angle of the highest energy conformer
dE: Energy difference between the highest and lowest energy conformers

4. CONCLUSIONS

In conclusion, docking studies are known to have pitfalls and there has been continuous effort towards overcoming these. Post-docking analysis using methods such as molecular dynamics simulations and free energy calculations, while being quite robust, are computationally expensive and time consuming. MMGB-SA method implemented in Schrodinger Suite was seen to be quite useful as a fast and reasonable alternative in rationalizing the observed experimental results, and may be incorporated as a routine post-docking analysis while making predictions based on docking. In the current scenario, MMGB-SA followed by quantum mechanics strain energy calculations and torsion angle drive studies provided insights into the possible reasons for inactivity of reverse pyrimidines in xanthine oxidase.

5. REFERENCES

[1] Eger B.T., Okamoto K., Enroth C., Sato M., Nishino T., Pai E.F., Nishino T., Purification, crystallization and preliminary X-ray diffraction studies of xanthine dehydrogenase and xanthine oxidase isolated from bovine milk, *Acta Crystallographica Section D,* 56, 1656-1658, **2000.**

[2] Borges F., Fernandes E., Roleira F., Progress Towards the Discovery of Xanthine Oxidase Inhibitors, *Current Medicinal Chemistry*, 9, 195-217, **2002.**
[3] Hille R., The Mononuclear Molybdenum Enzymes, *Chemical Reviews*, 96, 7, 2757-2816, **1996.**
[4] Cantu-Medellin N., Kelley E.E., Xanthine oxidoreductase-catalyzed reactive species generation: A process in critical need of reevaluation *Redox Biology***,** 1, 353-358, **2013.**
[5] Xia M., Dempski R., Hille R., The Reductive Half-reaction of Xanthine Oxidase, *The Journal of Biological Chemistry,* 274, 6, 3323–3330, **1999.**
[6] Mapa J.B., Pillinger M.H., New treatments for gout, *Current Opinion in Investigational Drugs*, 1, 5, 499-506, **2010.**
[7] Kim K.Y., Schumacher H.R., Hunsche E., Wertheimer A.I., Kong S.X., A Literature Review of the Epidemiology and Treatment of Acute Gout, *Clinical Therapeutics*, 25, 6, 1593-1617, **2003.**
[8] Eggebeen A.T., Gout: An Update, *American Academy of Family Physicians,* 76, 801-808, **2007.**
[9] Pacher P., Nivorozhkin A., Szabo C., Therapeutic Effects of Xanthine Oxidase Inhibitors: Renaissance Half a Century after the Discovery of Allopurinol, *Pharmacological Reviews*, 58, 1, 87–114, **2006.**
[10] Okamoto K., Eger B.T., Nishino T., Kondo S., Pai E.F., Nishino T., An Extremely Potent Inhibitor of Xanthine Oxidoreductase, *The Journal of Biological Chemistry*, 278, 3, 1848–1855, **2003.**
[11] Becker M.A., Schumacher H.R., Wortmann Jr., R.L., MacDonald P.A., Eustace D., Palo W.A., Streit J., Joseph-Ridge N., Febuxostat Compared with Allopurinol in Patients with Hyperuricemia and Gout, *New England Journal of Medicine*, 353, 23, 2450-2461, **2005.**
[12] Ernst M.E., Fravel M.A., Febuxostat: A Selective Xanthine-Oxidase/Xanthine-Dehydrogenase Inhibitor for the Management of Hyperuricemia in Adults With Gout, *Clinical Therapeutics,* 31, 11, 2503–2518, **2009.**
[13] Soni J.P., Parmar D.R., Sen D.J., Febuxostat: The New Generation novel xanthine oxidase Inhibitors, *Internationale Pharmaceutica Sciencia*, 1, 1, 107-115, **2011.**
[14] Takanoa Y., Hase-Aokia K., Horiuchia H., Zhaob L., Kasaharaa Y., Kondoa S., Becker M. A., *Life Sciences*, *76*, 1835–1847, **2005.**
[15] B-Rao C., Kulkarni-Almeida A., Katkar K.V., Khanna S., Ghosh U., Keche A., Shah P., Srivastava A., Korde V., Nemmani K.V.S., Deshmukh N.J., Dixit A., Brahma M.K., Bahirat U., Doshi L., Sharma R., Sivaramakrishnan H., Identification of novel isocytosine derivatives as xanthine oxidase inhibitors from a set of virtual screening hits, *Bioorganic & Medicinal Chemistry*, 20, 2930, **2012.**
[16] Lagunin A., Stepanchikova A., Filimonov D., Poroikov V., PASS: Prediction Of Activity Spectra For Biologically Active Substances, *Bioinformatics*, 16, 8, 747-748, **2000.**
[17] Khanna S., Burudkar S., Bajaj K., Shah P., Keche A., Ghosh U., Desai A., Srivastava A., Kulkarni-Almeida A., Deshmukh N.J., Dixit A., Brahma M.K., Bahirat U., Doshi L., Nemmani K.V., Tannu P., Damre A., B-Rao C., Sharma R., Sivaramakrishnan H., Isocytosine-based inhibitors of xanthine oxidase: Design, synthesis, SAR, PK and in vivo efficacy in rat model of hyperuricemia, *Bioorganic & Medicinal Chemistry Letters,* 22, 7543–7546, **2012.**
[18] Bajaj K., Burudkar S., Shah P., Keche A., Ghosh U., Tannu P., Khanna S., Srivastava A., Deshmukh N.J., Dixit A., Ahire Y., Damre A., Nemmani K.V., Kulkarni-Almeida A., B-Rao C., Sharma R., Sivaramakrishnan H., Lead optimization of isocytosine-derived xanthine oxidase inhibitors, *Bioorganic & Medicinal Chemistry Letters,* 23, 834–838, **2013.**
[19] *GLIDE, version 5.6*; Schrödinger, LLC: New York, NY, **2010.**
[20] Fukunari A., Okamoto K., Nishino T., Eger B.T., Pai E.F., Kamezawa M., Yamada I., Kato N., Y-700 [1-[3-Cyano-4-(2,2-dimethylpropoxy)phenyl]-1*H*pyrazole-4-carboxylic Acid]: A Potent Xanthine Oxidoreductase Inhibitor with Hepatic Excretion, *The Journal of Pharmacology and Experimental Therapeutics*, 311, 2, 519–528, **2004.**
[21] Sathisha K.R., Khanum S.A., Chandra J.N.N.S., Ayisha F., Balaji S., Marathe G.K., Gopal S., Rangappa K.S., Synthesis and xanthine oxidase inhibitory activity of 7-methyl-2-(phenoxymethyl)-5H-[1,3,4]thiadiazolo[3,2-a]pyrimidin-5-one derivatives, *Bioorganic & Medicinal Chemistry,* 19, 211-220, **2011.**
[22] Ishibuchi S., Morimoto H., Oe T., Ikebe T., Inoue H., Fukunari A., Kamezawa M., Yamadab I., Nakaa Y., Synthesis and Structure–Activity Relationships of 1-Phenylpyrazoles as Xanthine Oxidase Inhibitors, *Bioorganic & Medicinal Chemistry Letters*, 11, 879-882, **2001.**
[23] *PRIME, version 2.2*; Schrödinger, LLC: New York, NY, **2010.**
[24] *JAGUAR, version 5.5*; Schrödinger, LLC: New York, NY, **2014.**

© 2016 by the authors. This article is an open access article distributed under the terms and conditions of the Creative Commons Attribution license (http://creativecommons.org/licenses/by/4.0/).